Supplemental Material for "Piercing the Dirac spin liquid: from a single monopole to chiral states"

Sasank Budaraju,[1,2] Yasir Iqbal,[2] Federico Becca,[3] and Didier Poilblanc[1]

[1]*Laboratoire de Physique Théorique, Université de Toulouse, CNRS, UPS, France*
[2]*Department of Physics and Quantum Centre of Excellence for Diamond and Emergent Materials (QuCenDiEM), Indian Institute of Technology Madras, Chennai 600036, India*
[3]*Dipartimento di Fisica, Università di Trieste, Strada Costiera 11, I-34151 Trieste, Italy*

(Dated: July 8, 2023)

I. SU(N_f) MONOPOLE

Here, we generalize the investigation described in the main text by studying the behavior of monopole excitations for fermion flavors $N_f > 2$. For that purpose we consider the following SU(N_f) generalization of the Heisenberg Hamiltonian [S1]

$$\mathcal{H} = \sum_{\langle i,j\rangle} \sum_{\alpha\beta}^{N_f} c^\dagger_{i,\alpha} c_{i,\beta} c^\dagger_{j,\beta} c_{j,\alpha} \tag{S1}$$

with N_f even integer and $N_f/2$ fermions per site. Here, α, β are "spin" indices that take the values $\alpha, \beta = 1, 2, \ldots N_f$. For the standard SU(2) case, this is related to the Heisenberg Hamiltonian as

$$\mathbf{S}_i \cdot \mathbf{S}_j = \frac{1}{2} \sum_{\alpha,\beta} c^\dagger_{i,\alpha} c_{i,\beta} c^\dagger_{j,\beta} c_{j,\alpha} - \frac{1}{4} n_i n_j \tag{S2}$$

where

$$n_i = c^\dagger_{i,\uparrow} c_{i,\uparrow} + c^\dagger_{i,\downarrow} c_{i\downarrow} \,. \tag{S3}$$

The latter term in Eq. (S2) is just a constant in the subspace with one fermion per site.

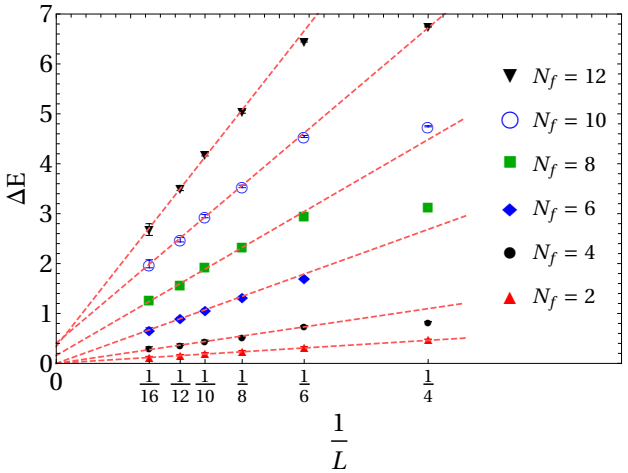

FIG. S1. Single-monopole gap as a function of $1/L$ for various values of N_f, along with best linear fits.

At the unprojected level, the expectation values of (S1) can be computed using Wick's theorem. The many-body wave function $|\Phi_0\rangle$ is constructed as a product of $N/2$ orbitals for each spin flavor:

$$|\Phi_0\rangle = \prod_{\alpha=1}^{N_f} \left(\prod_{x=1}^{N/2} \phi^\dagger_{x,\alpha} \right) |0\rangle \,, \tag{S4}$$

where $N = 3L^2$ is the number of sites. The (orthonormal) orbitals $\phi^\dagger_{x,\alpha}$ are obtained by diagonalizing the relevant free-fermion tight-binding model (either the Dirac or the monopole ansatz)

$$\phi^\dagger_{x,\alpha} = \sum_{j=1}^{N} U_{j,x} c^\dagger_{j,\alpha} \,, \tag{S5}$$

where U is the $N \times N$ eigenvector matrix. The unprojected expectation value

$$E_0 = \frac{\langle \Phi_0 | \, H \, | \Phi_0 \rangle}{\langle \Phi_0 | \Phi_0 \rangle} \tag{S6}$$

can be evaluated, using Eq. (S5), as

$$E_0 = -\sum_{\langle i,j\rangle} \left[N_f^2 |A_{i,j}|^2 + \frac{N_f}{4} \right] \tag{S7}$$

where

$$A_{i,j} = \sum_{x=1}^{N/2} U_{j,x} U^*_{i,x} \,. \tag{S8}$$

Thus the coefficients $A_{i,j}$ can be readily calculated from a real-space diagonalization of the tight-binding model. The single-monople gap is obtained by taking the difference between the case with one monopole (spread over the entire torus) and no monopoles (i.e., the Dirac state):

$$\Delta E_0 = -N_f^2 \sum_{\langle i,j\rangle} \left[|A^{\text{monopole}}_{i,j}|^2 - |A^{\text{Dirac}}_{i,j}|^2 \right] \,. \tag{S9}$$

For the projected wave functions, we use the Monte Carlo sampling to evaluate the variational energies corresponding to

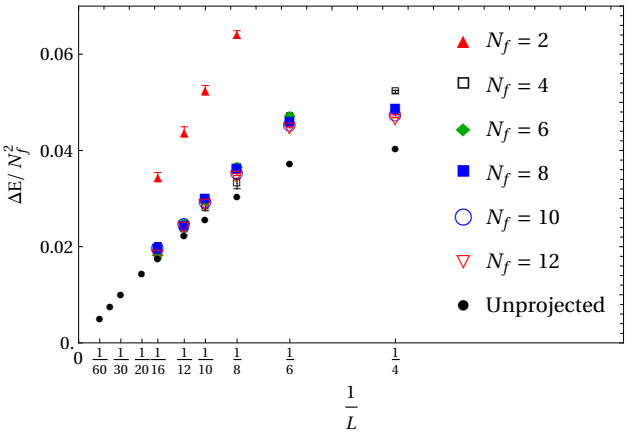

FIG. S2. Single-monopole energies scaled by N_f^2, shown along with the unprojected energy difference $\Delta E_0/N_f^2$ from Eq. (S9).

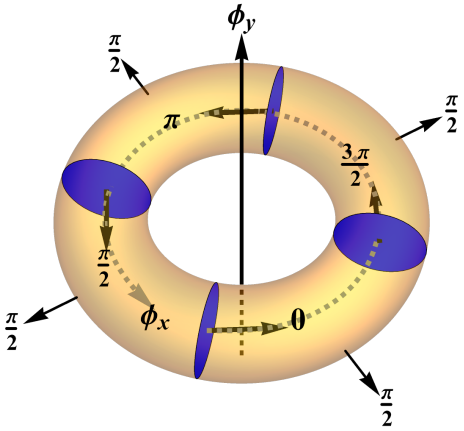

FIG. S3. Fluxes through (one set of) incontractible loops of the $L = 4$ torus for the monopole state. Also shown schematically are the angles ϕ_x and ϕ_y, which control boundary conditions.

the single monopole and the Dirac state (in both cases, the Gutzwiller projector imposes to have $N_f/2$ fermions per site).

The size scaling of the total monopole energy for $N_f = 2, 4, 6, 8, 10$, and 12 is shown in Fig. S1.

At first glance, the data for $N_f \geq 8$ would suggest a gapped monopole in the thermodynamic limit. However, after further investigation, we believe this to be a finite-size effect. Indeed, by scaling the projected energies by N_f^2, we observe that all the data (except $N_f = 2$) collapse perfectly on top of each other, see Fig. S2. Furthermore, there is very good agreement between the projected and the unprojected energies calculated from Eq. (S9), which increases with system size. Finally, we remark that the unprojected data indicates a gapless monopole only if large enough system sizes $L \geq 30$ are considered, which are very difficult to access for the projected wave functions.

II. MEAN FIELD MONOPOLE SPECTRUM AND BOUNDARY CONDITIONS

In the main text, we remarked that the two-fold degeneracy at the Fermi level upon adding the monopole flux on top of the Dirac state cannot be removed by changing the boundary conditions. Indeed, this is true for both the square and the Kagome lattice. Thus, the open shell at the Fermi level is an unavoidable consequence of the monopole flux. We also observed that in general (for large enough lattice sizes L), when more monopoles N_m are added, the degeneracy at the fermi level is $2 \times N_m$ for small values of N_m.

Since each plaquette has a flux $2\pi/L^2$ piercing it, the total flux through a cylindrical strip of the lattice containing L sites is $2\pi/L$, in contrast to the Landau gauge where it would have been a multiple of 2π. This necessarily implies non-trivial fluxes through the incontractible loops (marked in blue in figure S3) of the torus. As a result, translational symmetry is broken along *both* the lattice directions $\vec{a}_1$ and $\vec{a}_2$.

In general, for a $L \times L$ lattice, the fluxes through these loops are $0, 2\pi/L, 4\pi/L, \ldots$. A natural consequence of these non-trivial fluxes is that the boundary conditions ϕ_x, ϕ_y can be chosen modulo $2\pi/L$.

[S1] I. Affleck, Z. Zou, T. Hsu, and P. W. Anderson, SU(2) gauge symmetry of the large-U limit of the Hubbard model, Phys. Rev. B **38**, 745 (1988).